



CH9900038

PSI Ber. 98-11



PSI Bericht Nr. 98-11
September 1998
ISSN 1019-0643

Task Force Beschleunigerabfall

The PSIMECX medium-energy neutron activation
cross-section library Part III: Computational methods
for heavy nuclei

F. Atchison

30 - 49

Paul Scherrer Institut
CH - 5232 Villigen PSI
Telefon 056 310 21 11
Telefax 056 310 21 99

The PSIMECX medium-energy neutron activation cross-section library Part III: Computational methods for heavy nuclei

F. Atchison

Abstract

The PSIMECX library contains calculated nuclide production cross-sections for neutrons in the energy range about 2 to 800 MeV interacting with 72 stable isotopes of 24 elements.

^{12}C , ^{13}C , ^{16}O , ^{17}O , ^{18}O , ^{23}Na , ^{24}Mg , ^{25}Mg , ^{26}Mg , ^{27}Al , ^{28}Si , ^{29}Si , ^{30}Si , ^{31}P , ^{32}S , ^{33}S , ^{34}S , ^{36}S , ^{35}Cl , ^{37}Cl , ^{39}K , ^{40}K , ^{41}K , ^{40}Ca , ^{42}Ca , ^{43}Ca , ^{44}Ca , ^{46}Ca , ^{48}Ca , ^{46}Ti , ^{47}Ti , ^{48}Ti , ^{49}Ti , ^{50}Ti , ^{50}V , ^{51}V , ^{50}Cr , ^{52}Cr , ^{53}Cr , ^{54}Cr , ^{55}Mn , ^{54}Fe , ^{56}Fe , ^{57}Fe , ^{58}Fe , ^{58}Ni , ^{60}Ni , ^{61}Ni , ^{62}Ni , ^{64}Ni , ^{63}Cu , ^{65}Cu , ^{64}Zn , ^{66}Zn , ^{67}Zn , ^{68}Zn , ^{70}Zn , ^{92}Mo , ^{94}Mo , ^{95}Mo , ^{96}Mo , ^{97}Mo , ^{98}Mo , ^{100}Mo , ^{121}Sb , ^{123}Sb , ^{204}Pb , ^{206}Pb , ^{207}Pb , ^{208}Pb , ^{232}Th and ^{238}U .

The energy range covers essentially all transmutation channels other than capture. The majority of the selected elements are main constituents of normal materials of construction used in and around accelerator facilities and the library is, first and foremost, designed to be a tool for the estimation of their activation in wide-band neutron fields. This third report describes and discusses the calculational methods used for the heavy nuclei. The library itself has been described in the first report of this series and the treatment for the medium and light mass nuclei is given in the second.

Zusammenfassung

Die PSIMECX Datenbibliothek enthält berechnete Nuklid-Produktions-Wirkungsquerschnitte von Neutronen-induzierten Reaktionen im Energiebereich von 2 bis 800 MeV in den folgenden 72 stabilen Isotopen von 24 chemischen Elementen:

^{12}C , ^{13}C , ^{16}O , ^{17}O , ^{18}O , ^{23}Na , ^{24}Mg , ^{25}Mg , ^{26}Mg , ^{27}Al , ^{28}Si , ^{29}Si , ^{30}Si , ^{31}P , ^{32}S , ^{33}S , ^{34}S , ^{36}S , ^{35}Cl , ^{37}Cl , ^{39}K , ^{40}K , ^{41}K , ^{40}Ca , ^{42}Ca , ^{43}Ca , ^{44}Ca , ^{46}Ca , ^{48}Ca , ^{46}Ti , ^{47}Ti , ^{48}Ti , ^{49}Ti , ^{50}Ti , ^{50}V , ^{51}V , ^{50}Cr , ^{52}Cr , ^{53}Cr , ^{54}Cr , ^{55}Mn , ^{54}Fe , ^{56}Fe , ^{57}Fe , ^{58}Fe , ^{58}Ni , ^{60}Ni , ^{61}Ni , ^{62}Ni , ^{64}Ni , ^{63}Cu , ^{65}Cu , ^{64}Zn , ^{66}Zn , ^{67}Zn , ^{68}Zn , ^{70}Zn , ^{92}Mo , ^{94}Mo , ^{95}Mo , ^{96}Mo , ^{97}Mo , ^{98}Mo , ^{100}Mo , ^{121}Sb , ^{123}Sb , ^{204}Pb , ^{206}Pb , ^{207}Pb , ^{208}Pb , ^{232}Th und ^{238}U .

Der Energiebereich deckt alle Transmutationsreaktionen mit Ausnahme der Einfangsreaktionen ab. Der Grossteil der ausgewählten Elemente repräsentiert Bestandteile von benutzten Strukturmaterialien an Beschleunigeranlagen. Die vorliegende Datenbibliothek ist in erster Linie zur Berechnung der Aktivierung von Materialien durch Neutronen in einem sehr breiten Energiebereich ausgelegt.

Der vorliegende Bericht ist Teil III von 3 Berichten. Er beschreibt und diskutiert die Berechnungsmethodik für die schweren Nuklide. Die Datenbibliothek selbst ist in Teil I beschrieben. Die Behandlung der leichten und mittelschweren Nuklide ist in Teil II diskutiert. [M.J.]

Résumé

La bibliothèque de données PSIMECX contient des valeurs calculées pour les sections efficaces de production de nucléides dans des réactions induites par des neutrons de 2 à 800 MeV d'énergie et pour les 72 isotopes stables suivants de 24 éléments:

^{12}C , ^{13}C , ^{16}O , ^{17}O , ^{18}O , ^{23}Na , ^{24}Mg , ^{25}Mg , ^{26}Mg , ^{27}Al , ^{28}Si , ^{29}Si , ^{30}Si , ^{31}P , ^{32}S , ^{33}S , ^{34}S , ^{36}S , ^{35}Cl , ^{37}Cl , ^{39}K , ^{40}K , ^{41}K , ^{40}Ca , ^{42}Ca , ^{43}Ca , ^{44}Ca , ^{46}Ca , ^{48}Ca , ^{46}Ti , ^{47}Ti , ^{48}Ti , ^{49}Ti , ^{50}Ti , ^{50}V , ^{51}V , ^{50}Cr , ^{52}Cr , ^{53}Cr , ^{54}Cr , ^{55}Mn , ^{54}Fe , ^{56}Fe , ^{57}Fe , ^{58}Fe , ^{58}Ni , ^{60}Ni , ^{61}Ni , ^{62}Ni , ^{64}Ni , ^{63}Cu , ^{65}Cu , ^{64}Zn , ^{66}Zn , ^{67}Zn , ^{68}Zn , ^{70}Zn , ^{92}Mo , ^{94}Mo , ^{95}Mo , ^{96}Mo , ^{97}Mo , ^{98}Mo , ^{100}Mo , ^{121}Sb , ^{123}Sb , ^{204}Pb , ^{206}Pb , ^{207}Pb , ^{208}Pb , ^{232}Th et ^{238}U .

La gamme d'énergie recouvre toutes les réactions de transmutation sauf la capture. La plupart des éléments choisis sont parmi les constituants principaux des matériaux de construction utilisés autour des accélérateurs et la bibliothèque est tout spécialement destinée à faciliter l'estimation de l'activation de ces matériaux par les neutrons dans un domaine d'énergie très large.

Ce troisième rapport décrit et commente les méthodes de calcul utilisées pour les noyaux lourds. La bibliothèque elle-même a été décrite dans le premier rapport de cette série et le traitement des noyaux légers ou de masse intermédiaire est donné dans le deuxième. [M.P.]

Contents

1	Introduction	1
2	The modelling of heavy element interactions	1
2.1	Spallation-fission competition	4
2.2	Fission probabilities	4
2.3	Parameters for the scission products	5
2.4	Some comparisons between calculation and measurement	6
3	Some details about the computer codes	11
3.1	FUSSPOT	19
3.2	PFMPH	19
3.3	Notes on auxiliary routines	20
3.4	The EVAPF package	20
3.4.1	EVFINI	20
3.4.2	EVAPF1	21
3.4.3	EVAPF2	21
3.4.4	EVAPF	21
3.4.5	PUT & Co.	22
3.4.6	EVAPF4	22
3.4.7	EVAPF6	23
3.4.8	EVAPF7	23
3.4.9	Service routines	25
4	References	25

1 Introduction

The PSIMECX cross-section library [1] contains calculated cross-sections for nuclide production in neutron-nucleus interactions in the energy range about 2 to 800 MeV. The theoretical models and calculational methods used for light to medium mass isotopes (up to ^{123}Sb) have been described in a second report [2] (this will be referred to as 'II'); this report documents the extensions to the theoretical models and calculational methods for the treatment of heavy isotopes.

The main new aspect of interactions involving heavy nuclei is the significant contribution from fission. With suitably energetic projectiles, fission may be induced in most elements (for example, studies of Ce & Eu [3] and Ag [4] have been published). In light isotopes the fission probability is very low, also the products are in the same mass region as those from spallation. For the heavy elements, the fission probabilities are significant (up to 10% of the interaction cross-section for Pb and 50 to 80% for Th and U) and the fission products are well separated (see Figure 1).

Only one heavy element, Pb, is expected to be present in the radioactive waste from PSI-West in sufficient quantities to require inclusion in the cross-section library. Th and U have also been included because of the special significance of their interaction products.

Several treatments of medium energy particle induced fission have been made [5 - 12] but are mainly for use with Monte-Carlo transport codes in which the main concern is the influence of fission on production rates and spectra of fast neutrons; these are sensitive mainly to the gross effects - enhanced production due to binding energy interchange, the neutron richness of the fission products and hardening of the emission spectra due to the lighter mass of the fission products; there is no great sensitivity to the details of nuclide production.

Great significance is attached to obtaining 'complete' nuclide inventories in the calculations. Explicit numerical integration in the evaporation/fission calculation removes a major limitation to the calculational resolution; apart from setting a lower limit to cross-sections retained in the calculation, no artificial limitations on the nuclides produced is introduced. Specifically, the range of products possible is limited by energy considerations only, (a) the mass-table drip lines determine the limits of the neutron to proton ratio and (b) straightforward energy conservation limits the nucleon-loss. This explicit integration exposed irregularities in an earlier fission treatment [8] hidden by either or both of, the statistical fluctuations and limited resolution of Monte-carlo integration. This required the development of a new approach [13].

The report will start with a brief discussion of the new fission model. Fission apart, the majority of the physics of the interactions and their treatment are identical with that for lighter nuclei and as described in Sections 2 & 3 of II - technical problems force some changes and these will be discussed as appropriate.

2 The modelling of heavy element interactions

To make proper estimates of the residual nuclides, both the spallation and the fission products are required; in the relevant projectile energy range and for realistic target nuclei, the total fission probability will rarely exceed 80%. This means that both the fission and spallation products have significant production cross-sections. The main characteristic of medium energy nucleon interactions is the large range of intermediate nuclei from the primary interaction. Also, as evaporation in this heavy element region (where fission is also significant) is biased to neutron emission, neutron deficient intermediate states will occur in significant quantities in the evaporation chains. Simultaneously, the increasing fissility ($\frac{Z^2}{A}$) and decreasing excitation energy of these nuclei means that there will be a variable non-linear influence of fission on the spallation product cross-sections particularly in the mass region close to that of the target nucleus. A further feature is that α -particle evaporation is the main mechanism for reaching the spallation products at large displacements in charge and mass

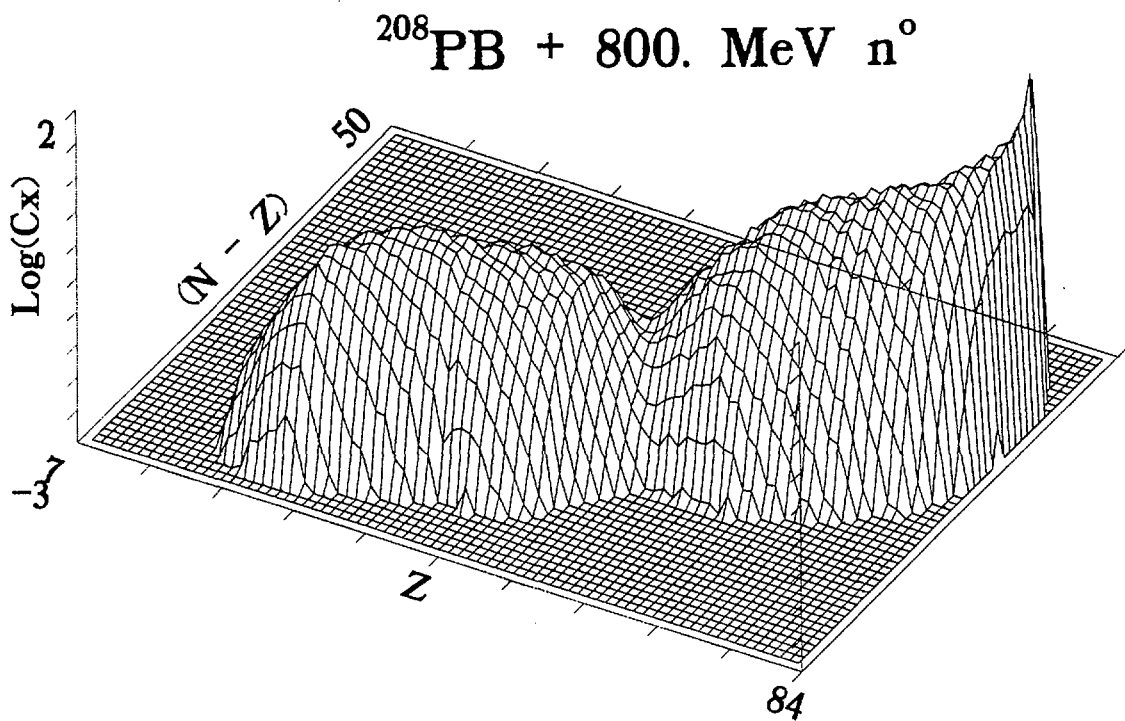
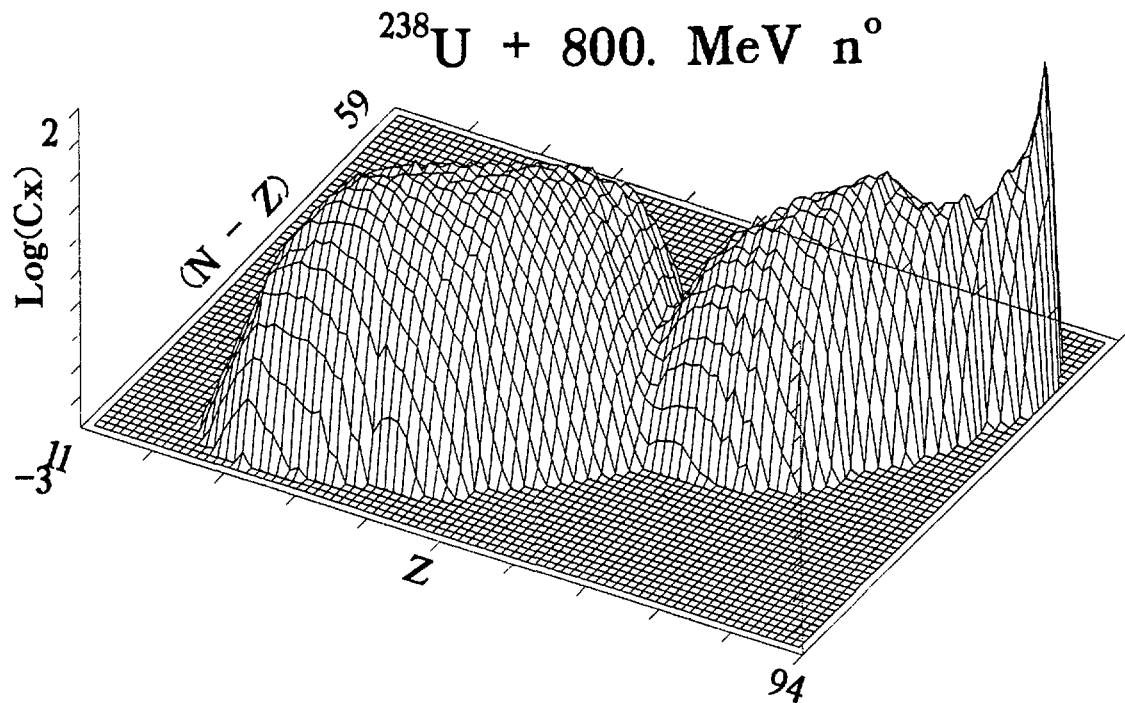


Figure 1: The projected distribution of product masses in the 800 MeV neutron induced fission of Uranium and Lead. The vertical axis is in units of Log_{10} of the cross-section in mb and the plot is in the Z vs $(N-Z)$ plane.

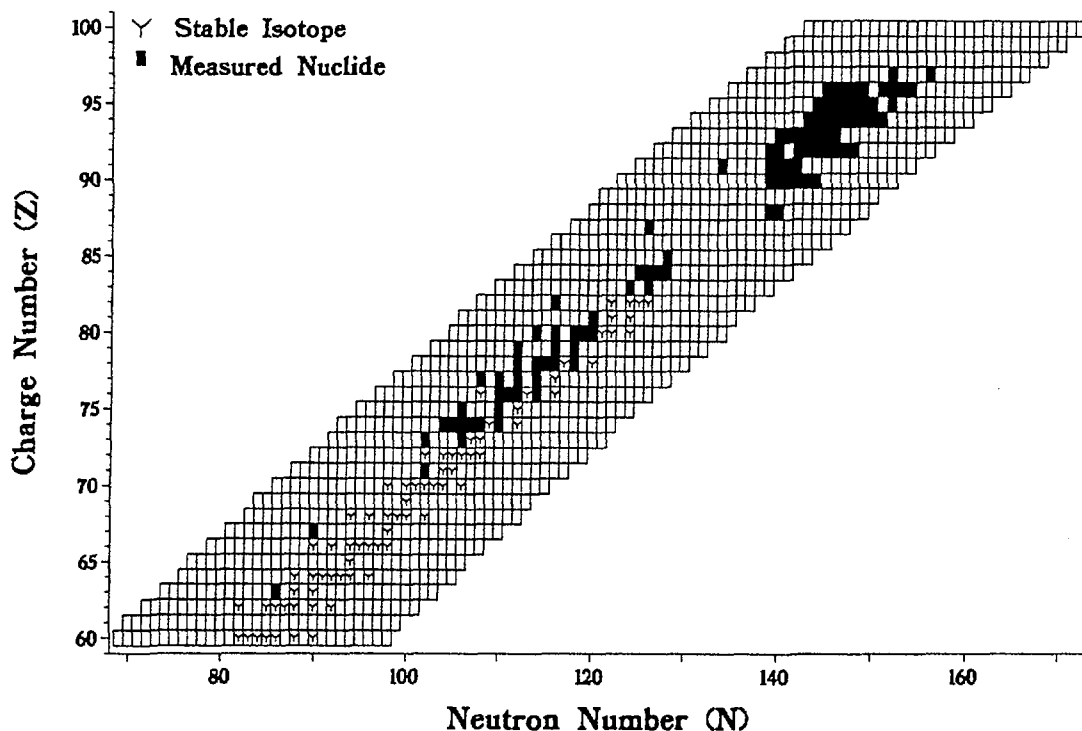


Figure 2: An N-Z diagram showing the nuclides for which fission probability measurements are available.

from the target nucleus. The quality of the fission modelling has a bearing on the spallation yields as well.

A medium energy nucleon induced fission model has to be able to treat a wide range of nuclear states; there are large variations in Z , A & E^* (particularly at the higher bombarding energies) for the intermediate state nuclei (see II, Section 2) and this is further increased as fission competes with evaporation at all stages of the de-excitation. Specifically, for the elements being calculated (Pb, Th & U), the treatment has to be able to handle all elements from Pu/Am ($Z = 94/95$) downwards and a large range of isotopes of each. Excitation energies will extend down from several hundred MeV to below fission thresholds. The principal areas of difficulty are:-

- the high sensitivity of calculated fission widths to the actual parameter values (both fission and evaporation widths are fast rising exponential functions of nuclear excitation energy),
- the leading parameters (level density parameters, fission barriers and neutron separation energies) have to form a self-consistent set for each nucleus to be treated,
- experimental data are comparatively sparse and so an interpolation/extrapolation scheme to generate the parameters for unmeasured nuclei is essential. The isotopes for which measured fission probabilities have been found are shown on an N-Z diagram (Nuclide chart) in Figure 2.

A fundamental assumption is that the fission probability for a given nucleus depends only on Z , A , E^* and J and not how this state is achieved. Hence, medium energy fission is the combination of the contributions from a wide range of nuclear states with the characteristics of the fission of the individual nuclear states identical with that achieved in other (and simpler to interpret) interactions.

Three additional factors made building the model difficult:

- (i) the behaviour of the fission probability for any single nucleus at high excitation energy is unknown

- (ii) the fission probabilities for nuclei between Bismuth and Thorium are unknown
- (iii) the fission probability for far off-stability nuclei throughout the heavy elements are unknown.

The overall treatment is in two parts, (i) the inclusion of fission as a competing channel during the de-excitation of the intermediate nuclei (spallation-fission competition) and (ii) the selection of the scission products and their evaporative de-excitation to the formation of the fission products.

The models and their parameterization will be summarised in the next two sub-sections (a full report on the fission treatment is available [13]) and followed by a short description of the codes together with how particular technical (computational) problems have been solved.

2.1 Spallation-fission competition

The new fission treatment [13] has been built into a code, EVAPF, which is based round the EVAPX code version using the Dostrovsky et al. [14, 15, 16] inverse reaction cross-section parameterization (see II Section 3.3.2) and, in contrast to the calculations for the medium mass nuclei, EVAPF is used to follow the complete de-excitation. The main considerations leading to this decision were:-

- Splitting at (say) 30 MeV excitation energy, as was done for the medium and light nuclei, and making the final de-excitation via the ALICE95 code would involve (i) introducing a consistent fission treatment (ALICE95 does include treatment of fission but attempting to obtain a smooth join is a task better avoided), (ii) building a coupling routine deep inside the ALICE95 code to pick up the parameters of the nucleus actually fissioning and (iii) because of the long evaporation chains, involve an unrealistically large number of de-excitation function data sets.
- The dominance of neutron emission in heavy nuclei and the reasonableness of the Dostrovsky parameterization for them.
- Implementation of fission has involved parameter adjustment using development versions of the actual code to be used. A simpler and faster code makes checking over a wide range of nuclei practicable.

The basic modification is small; the addition of code to compute the ratio of the channel widths for fission and neutron emission from which the fission probability relative to neutron emission (P_f^r) is obtained. The computation of the relative probabilities (r_1, \dots, r_6) for the evaporation of the six nucleon clusters (neutrons, protons, deuterons, tritons, ^3He nuclei and alpha particles) is unchanged. The final fission and neutron emission probabilities are then

$$P_f = P_f^r \times r_1 \quad ; \quad r_1 \leftarrow r_1 \times (1 - P_f^r)$$

This method is required because the individual fission and neutron widths are not calculated, only relative values.

2.2 Fission probabilities

Separate treatments are used depending on whether Z is above, or less than or equal to 87. In the $Z > 87$ region, the fission to neutron-emission width ratio is obtained directly from the Vandenbosch & Huizenga [17] correlation and for the lower Z region a simplified statistical model formulation is used for both the fission and neutron widths with the parameters' values - level density parameters for both neutron emission & fission and fission barriers - obtained from polynomial correlation formulae in terms of the fissility parameter.

In the high- Z region, fission barriers and appropriately adjusted effective neutron separation energies are obtained from a data set which covers 30 masses about the most stable for each element. This is necessary because both neutron separation energies and fission barriers are all about the same size

(a variation of 1 or 2 MeV about $\approx 6\frac{1}{2}$ MeV), which implies that any ‘formulae’ would need to be accurate to about 100 keV in 2 GeV otherwise difficulties would be encountered, for instance, in correctly accounting for fissile isotopes.

2.3 Parameters for the scission products

The fission products’ contribution to the nuclide production requires the selection of the mass, charge and excitation energy for the fragments at scission and then their de-excitation by evaporation to the ground state.

The production cross-sections for the fission products are given by

$$\sigma_f \cdot P(Z_1, A_1, \nu_1, Z_2, A_2, \nu_2)$$

where σ_f is the fission cross-section and $P(\dots)$ is the probability of a scission into two fragments, $[Z_1, A_1, E_1^*]$ and $[Z_2, A_2, E_2^*]$, that subsequently evaporate ν_1 and ν_2 nucleons respectively. Two basic assumptions are made:-

- (i) The scission is complete and into two fragments. That is (a) $Z_1 + Z_2 = Z_f$ and $A_1 + A_2 = A_f$, where Z_f and A_f are the charge and mass of the fissioning nucleus and (b) the energy partitioning is of the binding of the parent nucleus $[Z_f, A_f]$ and its excitation to the binding, recoil kinetic and excitation energies of the two scission fragments.
- (ii) The probability function, $P(\dots)$, is separable into (coupled) functions

$$P(\dots) = Q(Z_f, A_f, E_f^*; A_1) \cdot R(Z_f, A_f, E_f^*, A_1; Z_1) \cdot S(Z_f, A_f, E_f^*, A_1, Z_1; E_1^*, E_2^*)$$

where the function $Q(\dots)$ when supplied with the state of the fissioning nucleus gives the probability for the fragment of mass A_1 , $R(\dots)$, given in addition the fragment mass A_1 , returns the probability for an associated charge Z_1 and the function $S(\dots)$ gives the excitation energies. The form of these functions is discussed in Reference 13.

For any one fissioning system $[Z_f, A_f, E_f^*]$, the contribution from all scissions above a pre-selected lower cross-section limit are selected in the order mass, charge and finally excitation energy (which implicitly includes recoil kinetic energy). That is, the selection for a given fissioning system is over loops nested five deep (the outer two being over the states, $[Z_f, A_f]$ and E_f^* , of the nuclei undergoing scission) each of which has a limited “length” set by the size of the minimum significant probability alone.

Some features of the various functions are as follows:-

- The mass split has two clearly identified competing forms, symmetric and asymmetric, so that the relative probabilities of the two splits and the parameters for appropriate distribution functions, with their dependence on the state $[Z_f, A_f, E_f^*]$ of the fissioning nucleus are required. The functional form chosen is:-

$$\frac{\Gamma_{asym}}{\Gamma_{symm}} = C_1 \cdot \exp^{-C_2 \cdot E_f^*}$$

where E_f^* is the excitation of the scissioning nucleus and the parameter values are derived from available experimental data.

The asymmetric scission’s mass distribution is based on the cluster model [18, 19] and the symmetric, on a flat top with Gaussian edges, as suggested by available experimental data.

- The dispersion of the charge between the fragments is not clearly definable from experimental evidence. The form implemented is a simple Gaussian function. The choice of mean charge is based on ‘equal’ distance from the valley of stability.

Experimental measurements and calculations indicate that a constant standard deviation of 0.78 charge units is appropriate.

- The energy to be dispersed is the binding and excitation of the nucleus undergoing scission and this is to be transferred to the binding, recoil and excitation of the two fragments.

The recoil kinetic energy comes from the Coulomb repulsion between the fragments at scission. As of the order of 80% of the energy interchange in low excitation systems is to the recoil, a rather precise estimate for this is required if the correct excitation, and hence post-scission evaporation to the correct fission product, is to be obtained.

- Measured fragment kinetic energy distributions show an intrinsic distribution (i.e. it is not generated by the charge split variation) which is Gaussian in form and of FWHM 15%.

Because of energy conservation, this means that this variation determines the distribution of the excitation energy; that is, the probability of having one fragment with an excitation in the interval E^* to $E^* + dE^*$ (where dE^* is the width of the energy bin used in the numerical integration) is determined by the total recoil kinetic energy that it fixes:- If fragment 1 has an excitation energy E_1^* then, because of 'equal amount per nucleon', fragment 2 must have an excitation energy of

$$\frac{A_2}{A_1}[E_1^* - E_t^*(A_1)] + E_t^*(A_2)$$

2.4 Some comparisons between calculation and measurement

Fairly extensive comparisons with experimental results are included in Reference 13, so only a few selected figures will be included here.

- The excitation functions for neutron induced fission over the energy range 0.01 to 30 MeV for ^{232}Th and ^{238}U are shown in Figure 3. The experimental results are represented by the curves from the ENDF/B-IV neutron cross-section library [20] (ENDF/B-IV data extend to only 20 MeV), experimental measurements digitised from the graphs in BNL-325 [21] and the probabilities corresponding to the first chance fission channel measured by direct-reactions [22, 23] converted to cross-section using the Optical-Model.

The calculations reproduce many of the features of the cross-sections rather closely.

- Calculated and measured values for (i) $^{232}\text{Th}(n,2n)^{231}\text{Th}$ (ii) $^{238}\text{U}(n,2n)^{237}\text{U}$ and (iii) $^{238}\text{U}(n,3n)^{236}\text{U}$, are shown in Figure 4. Experimental results are from ENDF/B-IV [20] and BNL-325 [21].
- Calculated variations of fission cross-section with proton energy agree quite well with measured values. Values for ^{238}U [24 - 30], ^{209}Bi [25, 28, 31] and ^{nat}Pb [28] are shown in Figure 5 to 7.

A systematic measurement of the variation with target isotope of the proton induced fission of Uranium was carried out by Boyce et al. [32]. The experimental results include the relative contribution from the various Np isotopes to the fission probability. The results for ^{238}U bombardment are as follows:-

Proton Energy (MeV lab.)	Measured Values			Calculated Values			
	^{239}Np	^{238}Np	^{237}Np	^{239}Np	^{238}Np	^{237}Np	^{236}Np
5	1.0			1.0			
10	0.55	0.45		0.62	0.38		
15	0.43	0.37	0.20	0.542	0.349	0.107	
20	0.45	0.34	0.21	0.507	0.327	0.165	0.006

The values are in reasonable agreement.

- The procedure for the selection of the post-scission parameters gives a rather close representation of experimental results. The 2-D distribution of kinetic energy and mass of the scission

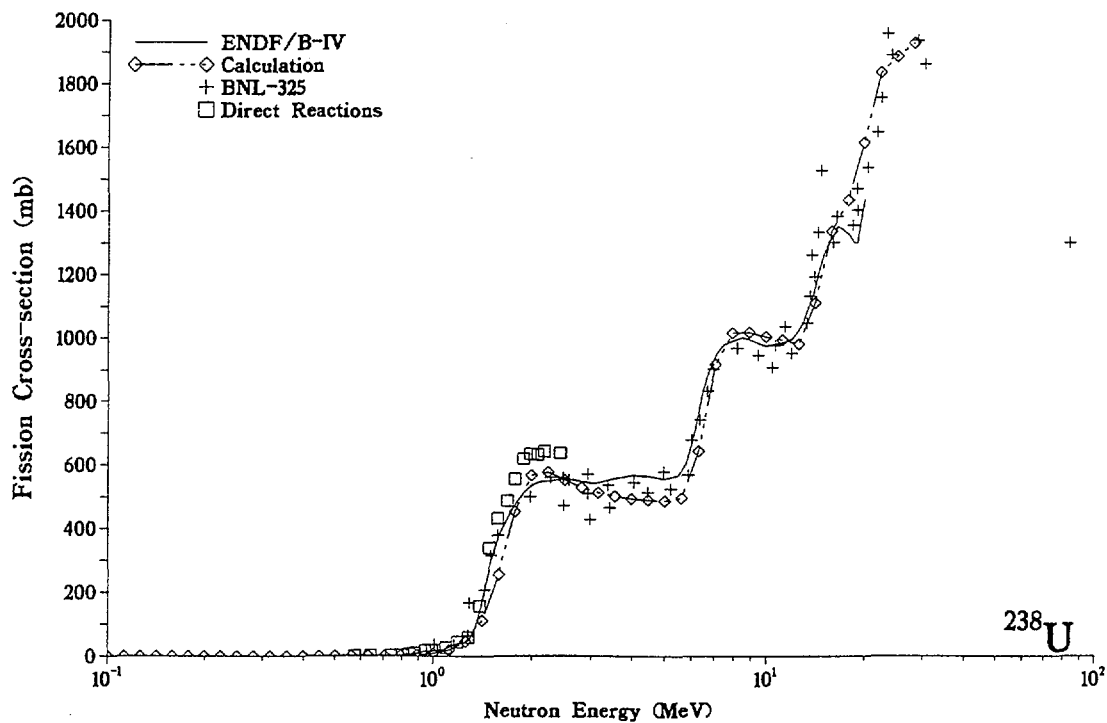
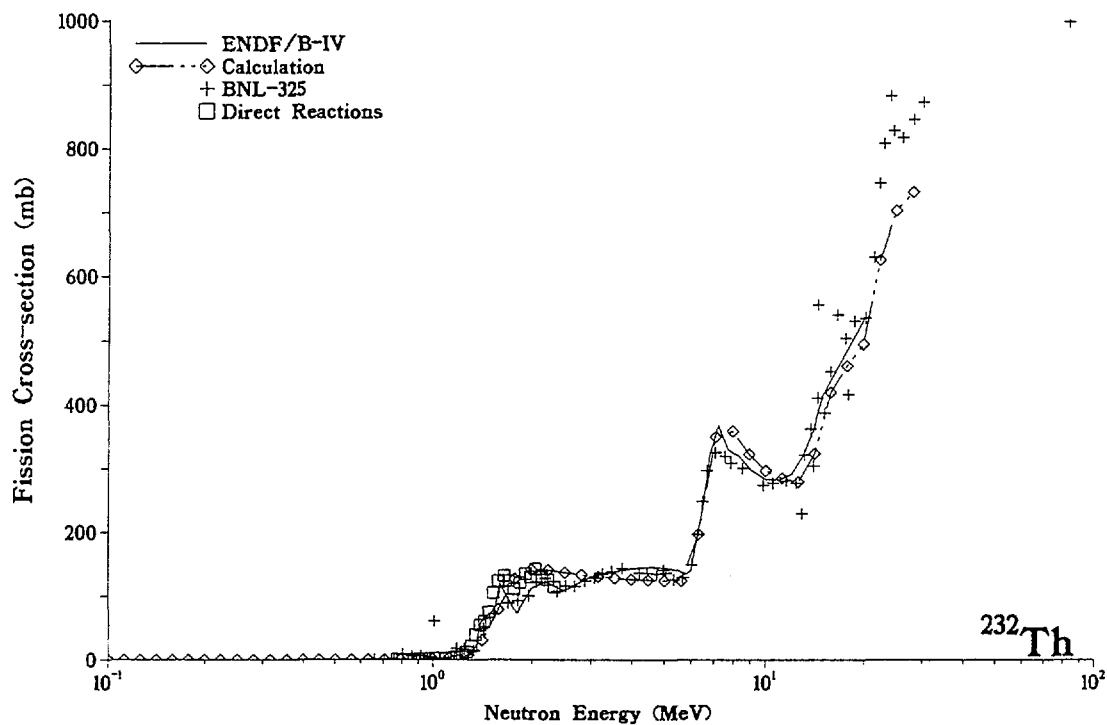


Figure 3: The total fission cross-section for neutron interactions with ^{232}Th and ^{238}U in the energy range 0.1 to 30 MeV. The calculated results are given by diamonds connected by double-dash lines, the measured data are represented by (i) the values in the ENDF/B-IV library [20] (the full line) (ii) data digitised from the BNL-325 curves (crosses) and (iii) the direct reaction measured fission probabilities converted to cross-section using the total cross-section as calculated with the Optical-Model (squares).

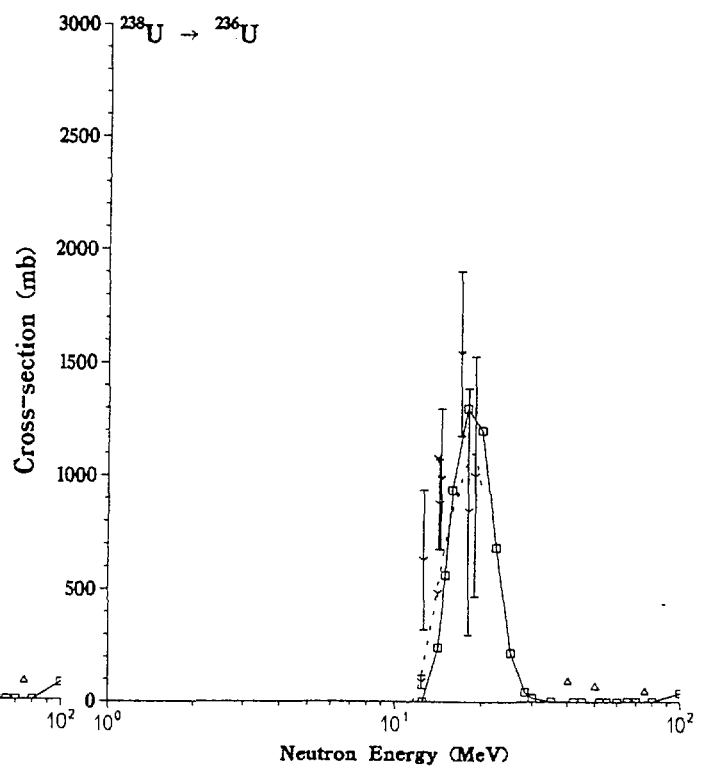
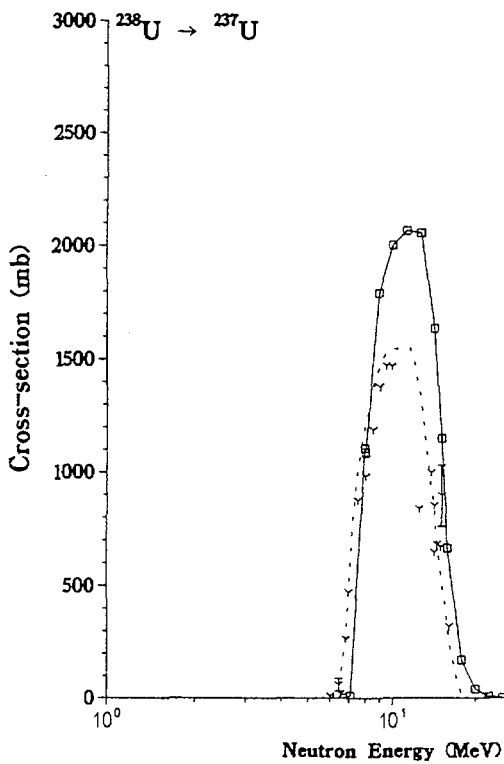
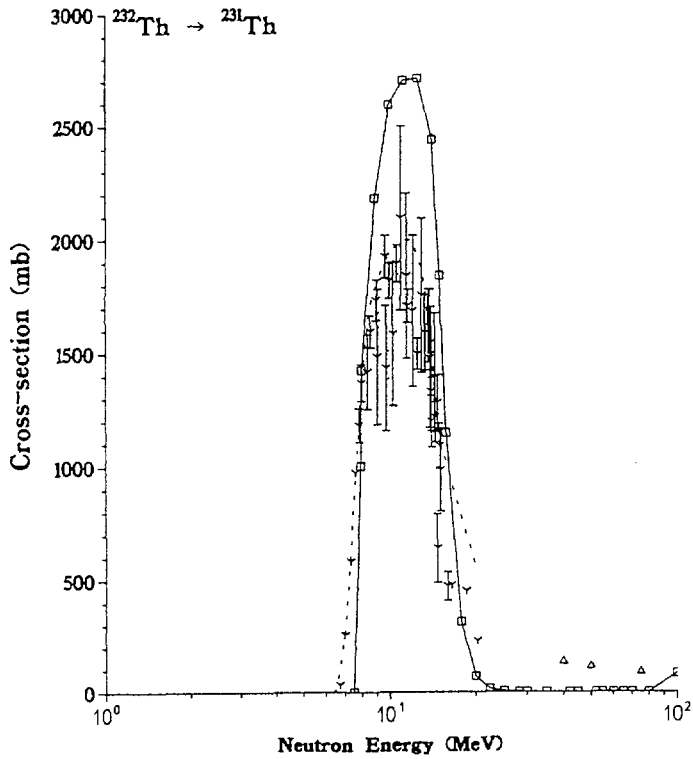


Figure 4: Excitation functions for the reactions (i) $^{232}\text{Th}(n,2n)^{231}\text{Th}$, (ii) $^{238}\text{U}(n,2n)^{237}\text{U}$ and (iii) $^{238}\text{U}(n,3n)^{236}\text{U}$ in the energy range 0.1 to 30 MeV. The calculated results are shown as squares connected by solid lines and the measured data are represented by (i) the values in the ENDF/B-IV library [20] as a dashed line and (ii) spot values digitised from the BNL-325 [21] curves (3-leaf stars).

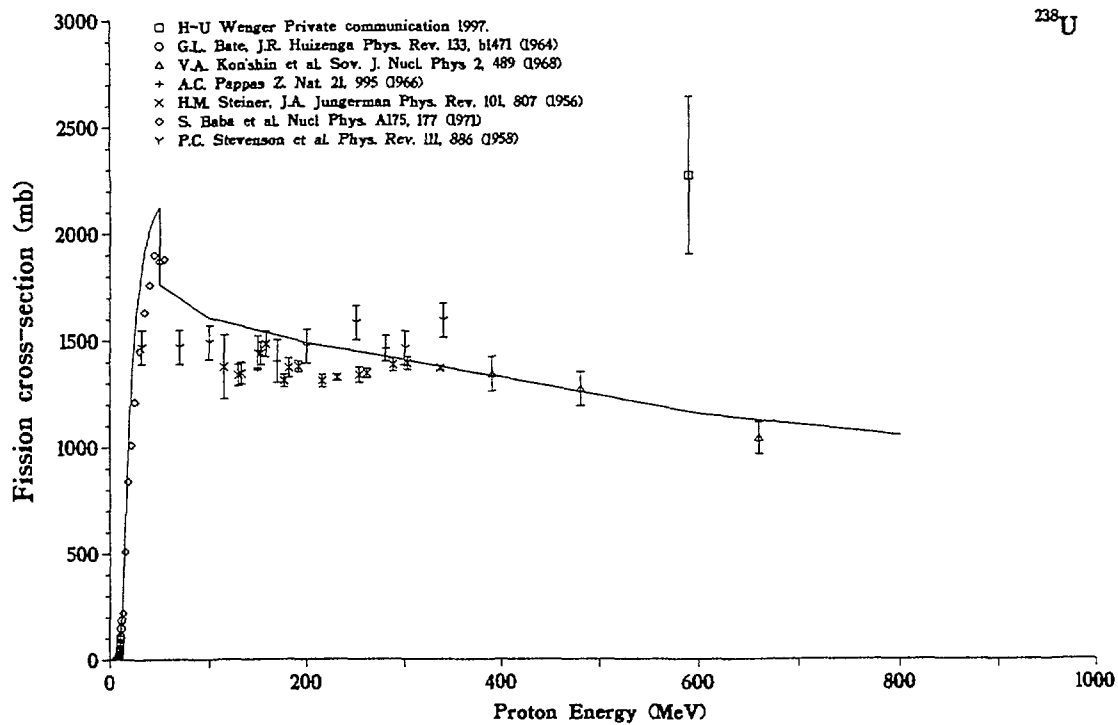


Figure 5: The total fission cross-section for proton interactions with ^{238}U in the energy range 0 to 800 MeV.

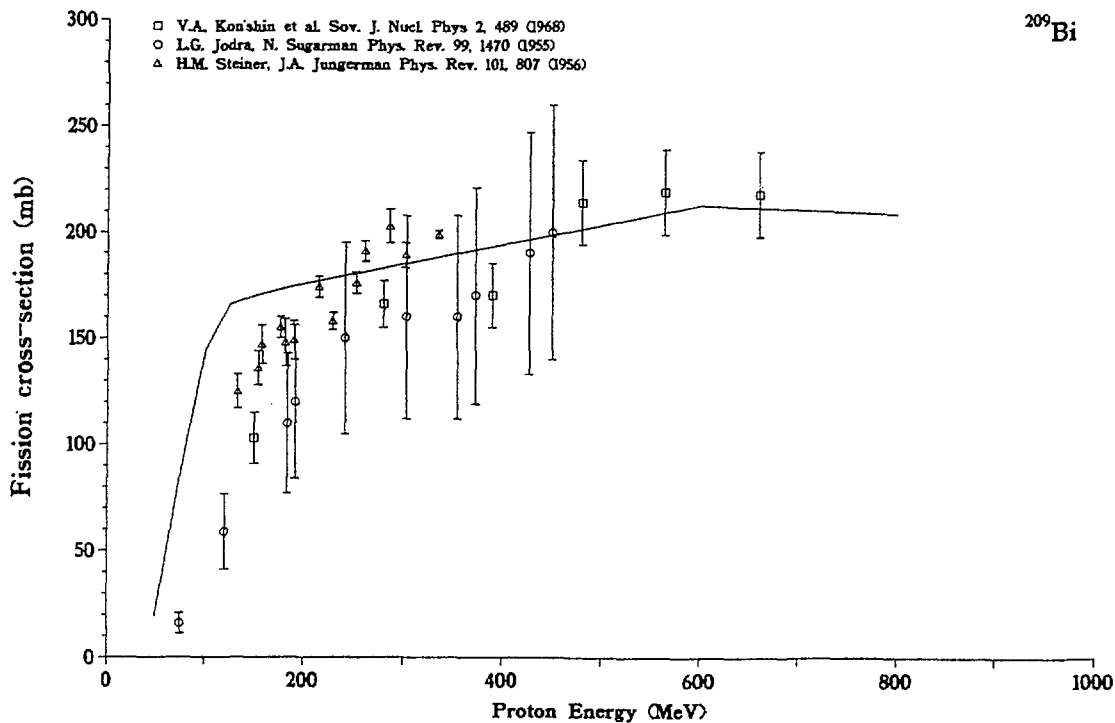


Figure 6: The total fission cross-section for proton interactions with ^{209}Bi in the energy range 0 to 800 MeV.

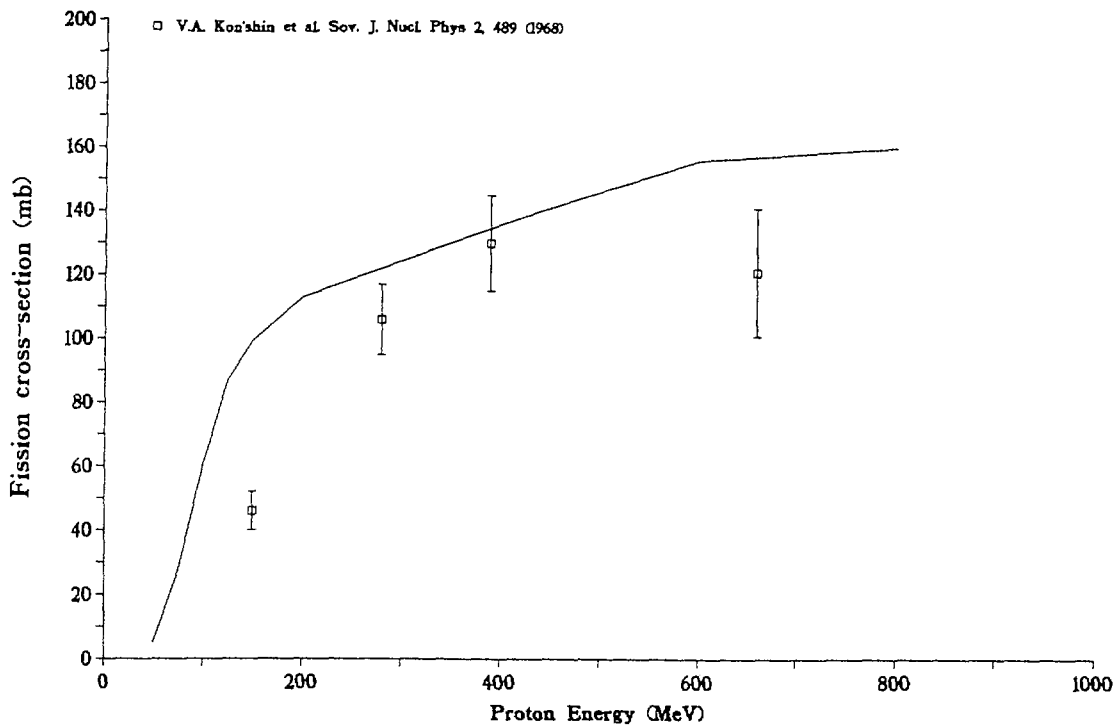


Figure 7: The total fission cross-section for proton interactions with ^{nat}Pb in the energy range 0 to 800 MeV.

products for fission induced by 13 MeV proton bombardment of ^{226}Ra is shown in Figure 8 and compares very well with the measured values of Konecny & Schmitt [33]. The calculated and measured fission cross-sections are in less good agreement (110 mb calculated, 34 ± 16 mb measured).

- A selection of 6 fission mass distributions (post scission de-excitation is included) together with measured values are shown in Figs 9 to 14. Because of the wide range of cross-section values (from μb to 100 mb), the results are shown both on a linear and a logarithmic scale.
1. Mass distributions for neutron induced fission; ^{232}Th at 0.5 MeV, ^{235}U with thermals and ^{238}U and 14 MeV. The experimental results come from the ENDF/B-IV data library [20]. The values are for the probabilities (the production cross-section divided by the fission cross-section and hence normalised to 200%). The agreement is as satisfactory as can be expected. A comparison of calculated and measured neutron yields is also satisfactory:-

Reaction	Calculated	Experimental
$^{232}\text{Th} + \frac{1}{2} \text{ MeV } n^{\circ}$	2.57	1.93
$^{233}\text{U} + \text{Therm. } n^{\circ}$	2.30	2.49
$^{235}\text{U} + \text{Therm. } n^{\circ}$	2.61	2.42
$^{235}\text{U} + \frac{1}{2} \text{ MeV } n^{\circ}$	2.67	2.48
$^{235}\text{U} + 14 \text{ MeV } n^{\circ}$	3.63	4.33
$^{238}\text{U} + \frac{1}{2} \text{ MeV } n^{\circ}$	2.40	2.39
$^{238}\text{U} + 14 \text{ MeV } n^{\circ}$	4.09	4.50
$^{237}\text{Np} + \text{Therm. } n^{\circ}$	2.72	2.74
$^{239}\text{Pu} + \text{Therm. } n^{\circ}$	2.85	2.87
$^{239}\text{Pu} + \frac{1}{2} \text{ MeV } n^{\circ}$	2.91	2.95
$^{241}\text{Am} + \text{Therm. } n^{\circ}$	2.96	3.22
$^{241}\text{Pu} + \frac{1}{2} \text{ MeV } n^{\circ}$	3.17	2.93

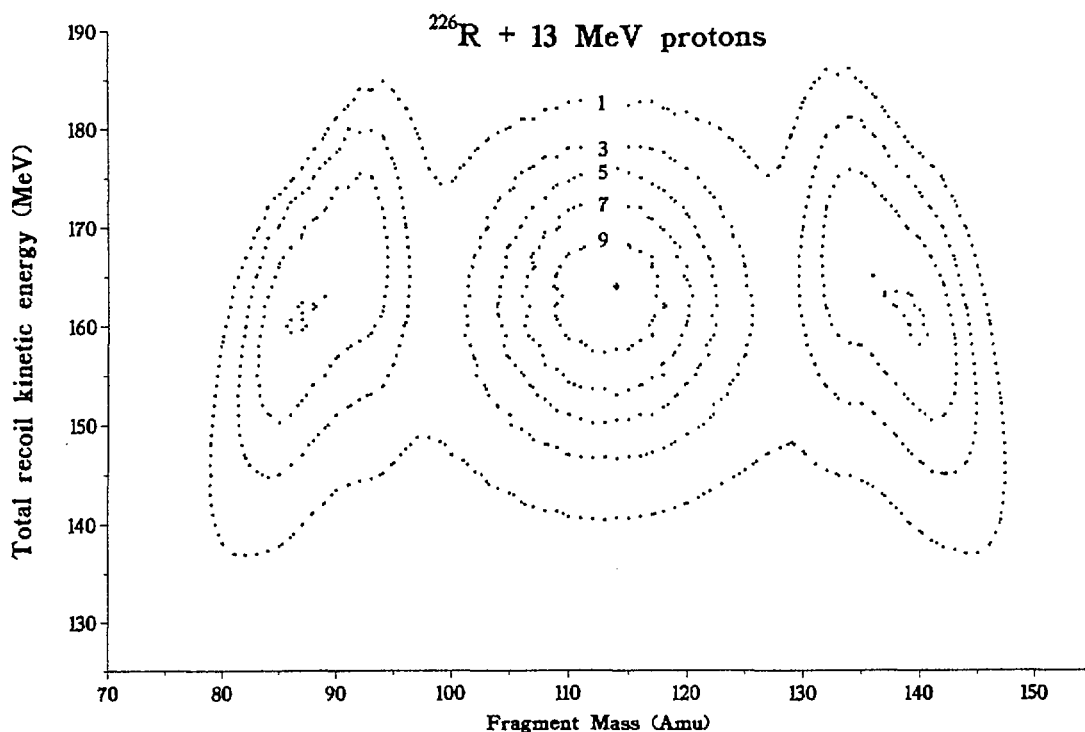


Figure 8: The variation of total kinetic energy with fragment mass in the 13 MeV proton induced fission of ^{226}Ra . The contours are in units of $10^{-4} \text{ MeV}^{-1} \text{ amu}^{-1}$ and may be compared with the measured values of Konecny & Schmitt [33].

2. Absolute mass production cross-sections for the fissions accompanying the bombardment of ^{238}U with protons of energy in the region 10 to 590 MeV. Measurements have been made by Stevenson et al. [26], Rudstam & Pappas [6], Pappas [29], Baba et al. [35] and Wenger [30]. Values at proton energies of 31 and 340 MeV are shown in Figures 12 and 13.
3. Absolute fission product cross-sections for 41.9 MeV α -particle bombardment of ^{197}Au have been measured by Neuzil & Fairhall [34]. This is the only example for the mass distribution from a comparatively light fissioning system found. The calculated and measured values are shown in Figure 14.

Some of the spallation products have been measured by Lindner & Osborne [36] for 340 and 200 MeV proton interactions (the values at 340 MeV are included in Figure 13).

3 Some details about the computer codes

The calculations have been carried out using either of two 'main' codes that invoke the new evaporation plus fission package. A brief description of these will be given first and then some details of the package members. Apart from some book-keeping information, the main routines produce no particularly useful output; the calculational results come from the EVAPF package and will be summarised in the appropriate sections.

Fission of ^{232}Th by 0.5 MeV Neutrons

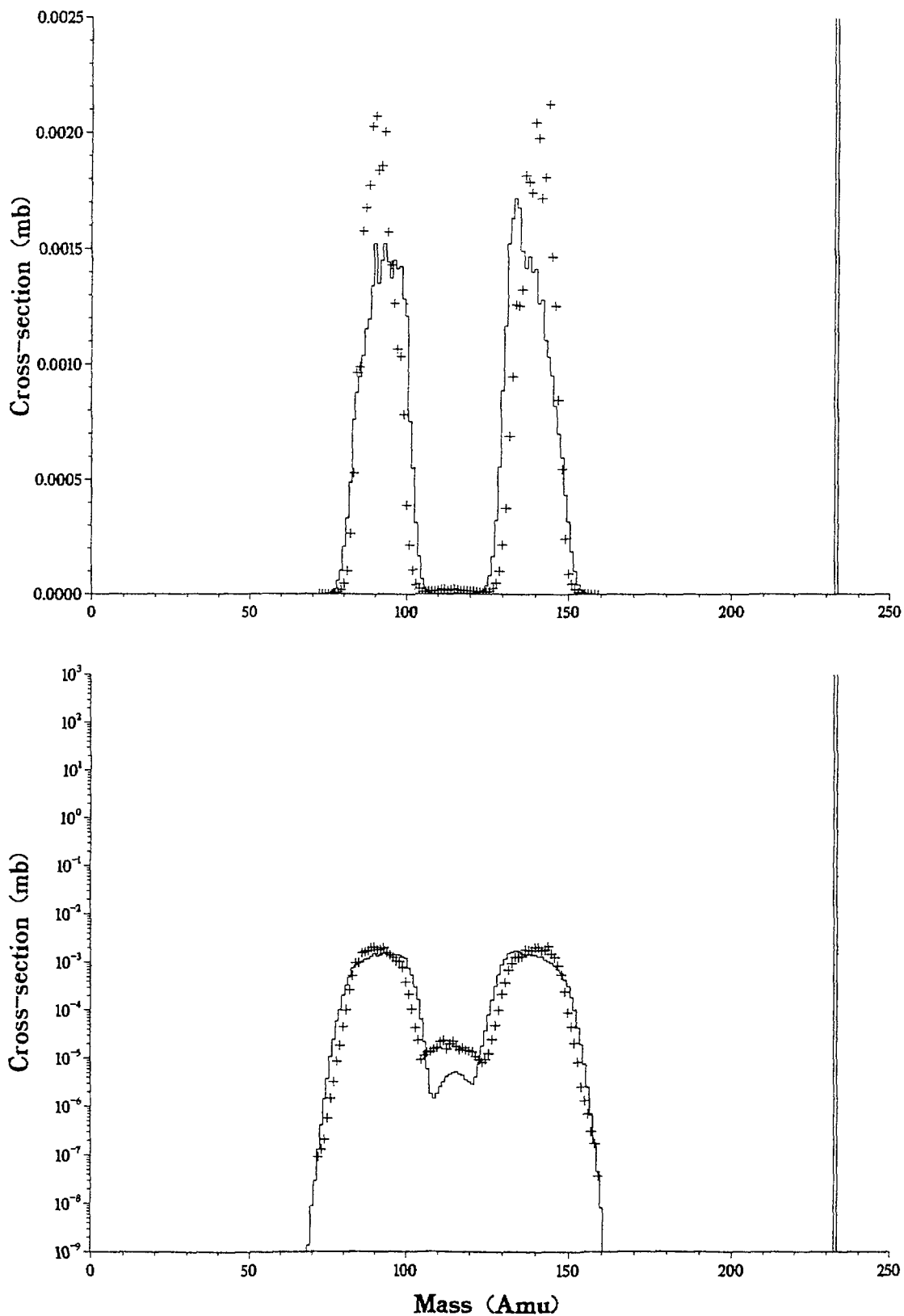


Figure 9: Calculated mass production cross-sections for 0.5 MeV neutron induced fission of ^{232}Th (histogramme). The 'experimental' results (crosses) are represented by values from the ENDF/B-IV library [20].

Fission of ^{235}U by Thermal Neutrons

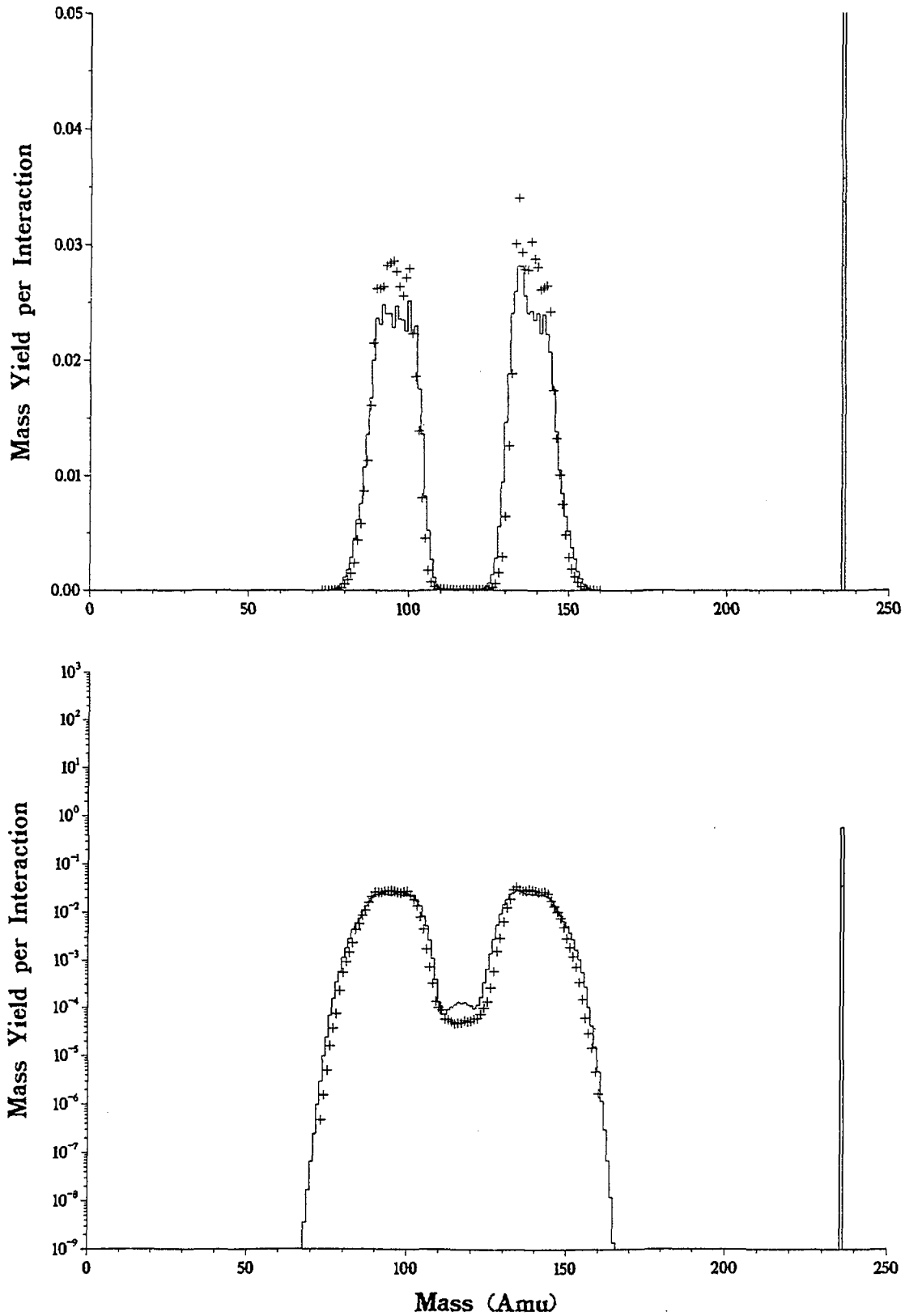


Figure 10: The calculated mass yield distribution for thermal neutron induced fission of ^{235}U (histogramme). The 'experimental' results (crosses) are represented by values from the ENDF/B-IV library [20].

Fission of ^{238}U by 14.0 MeV Neutrons

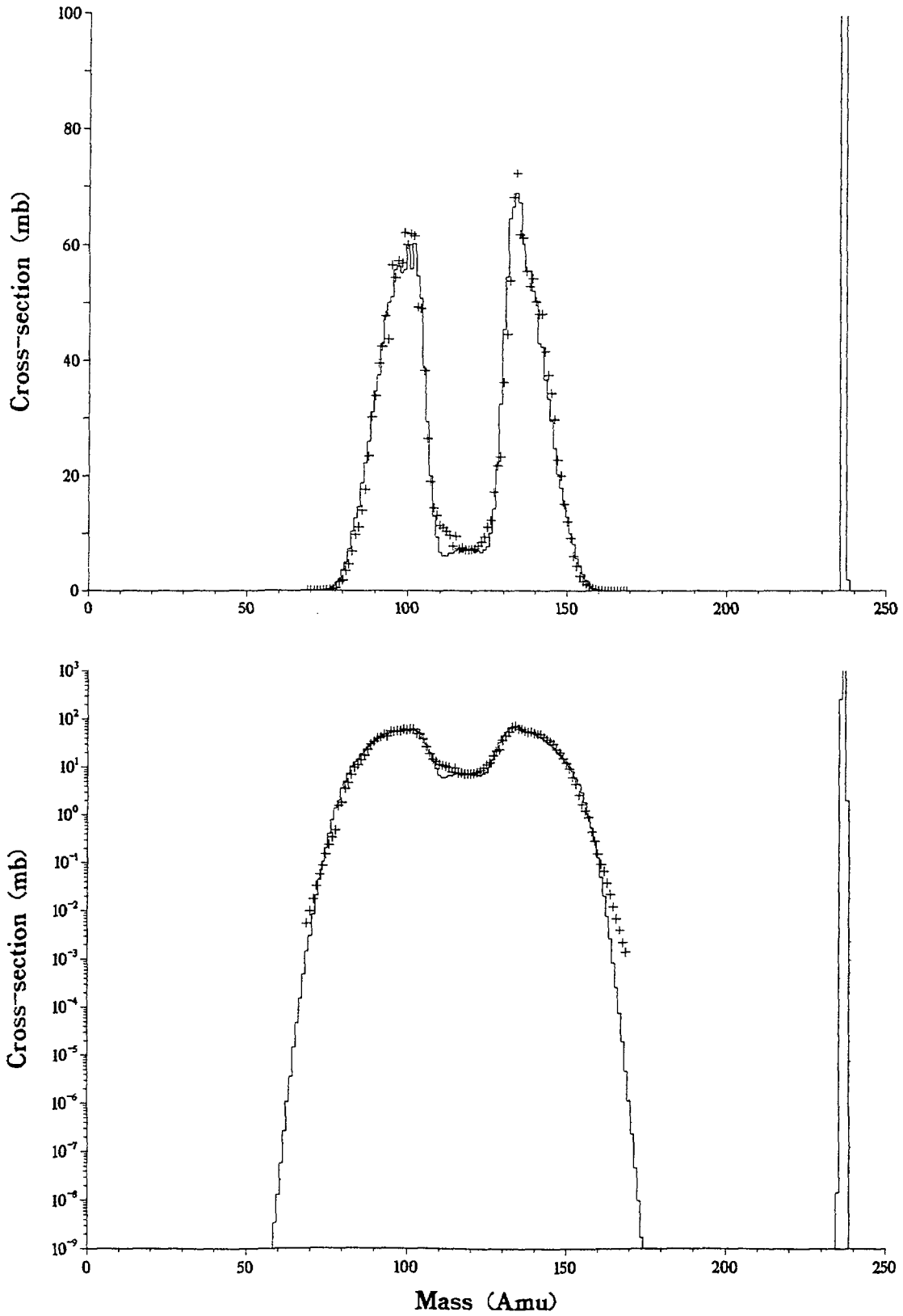


Figure 11: The calculated mass production cross-section for fission induced by 14 MeV neutrons in ^{238}U (histogramme). The 'experimental' results (crosses) are represented by values from the ENDF/B-IV library [20].

Fission of ^{238}U by 31.0 MeV Protons

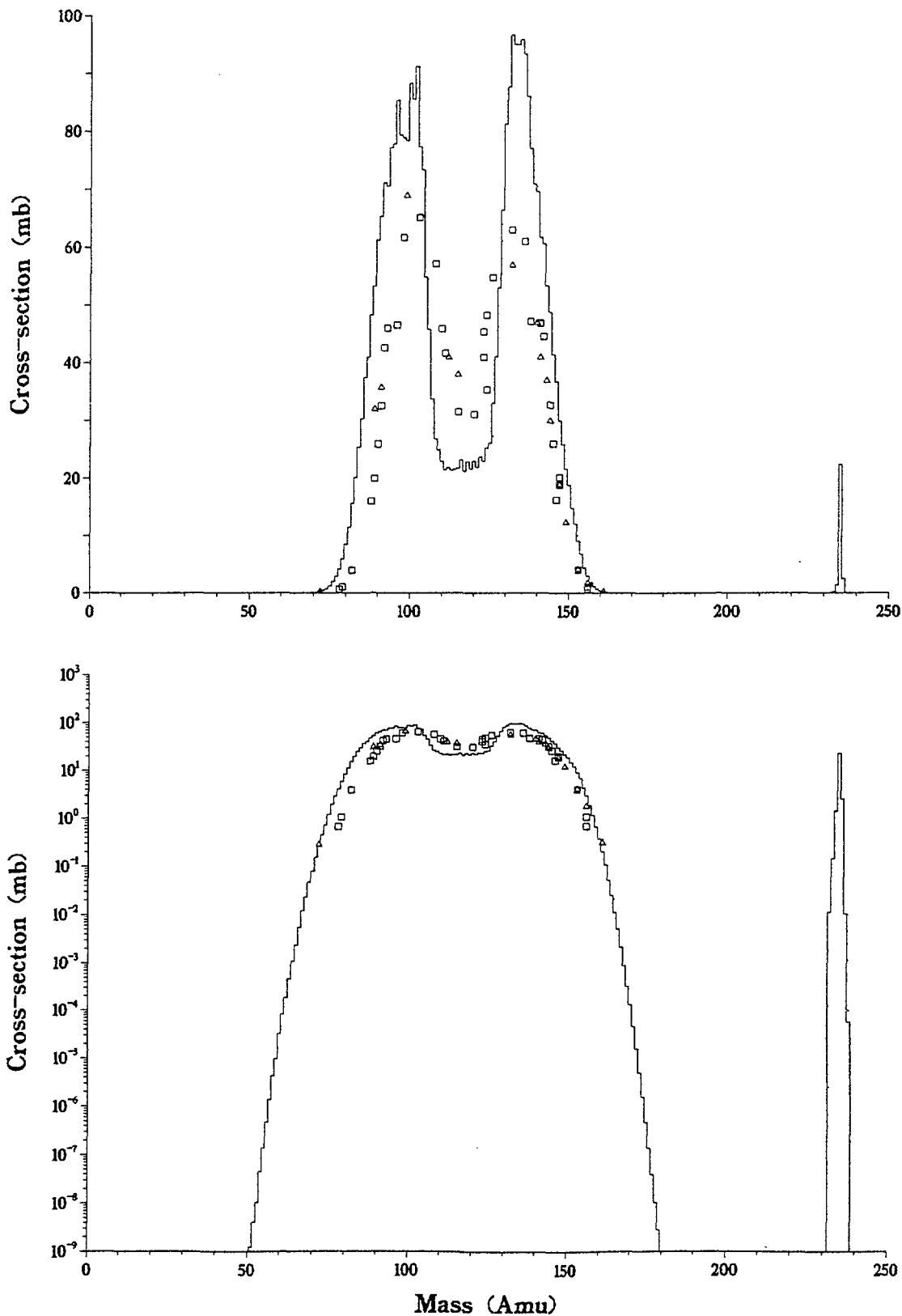


Figure 12: The calculated mass production cross-sections from fissions induced in ^{238}U by 31 MeV protons. The experimental results are from Stevenson et al. [26] (32 MeV - squares) and Baba et al. [35] (30 MeV - triangles).

Fission of ^{238}U by 340.0 MeV Protons

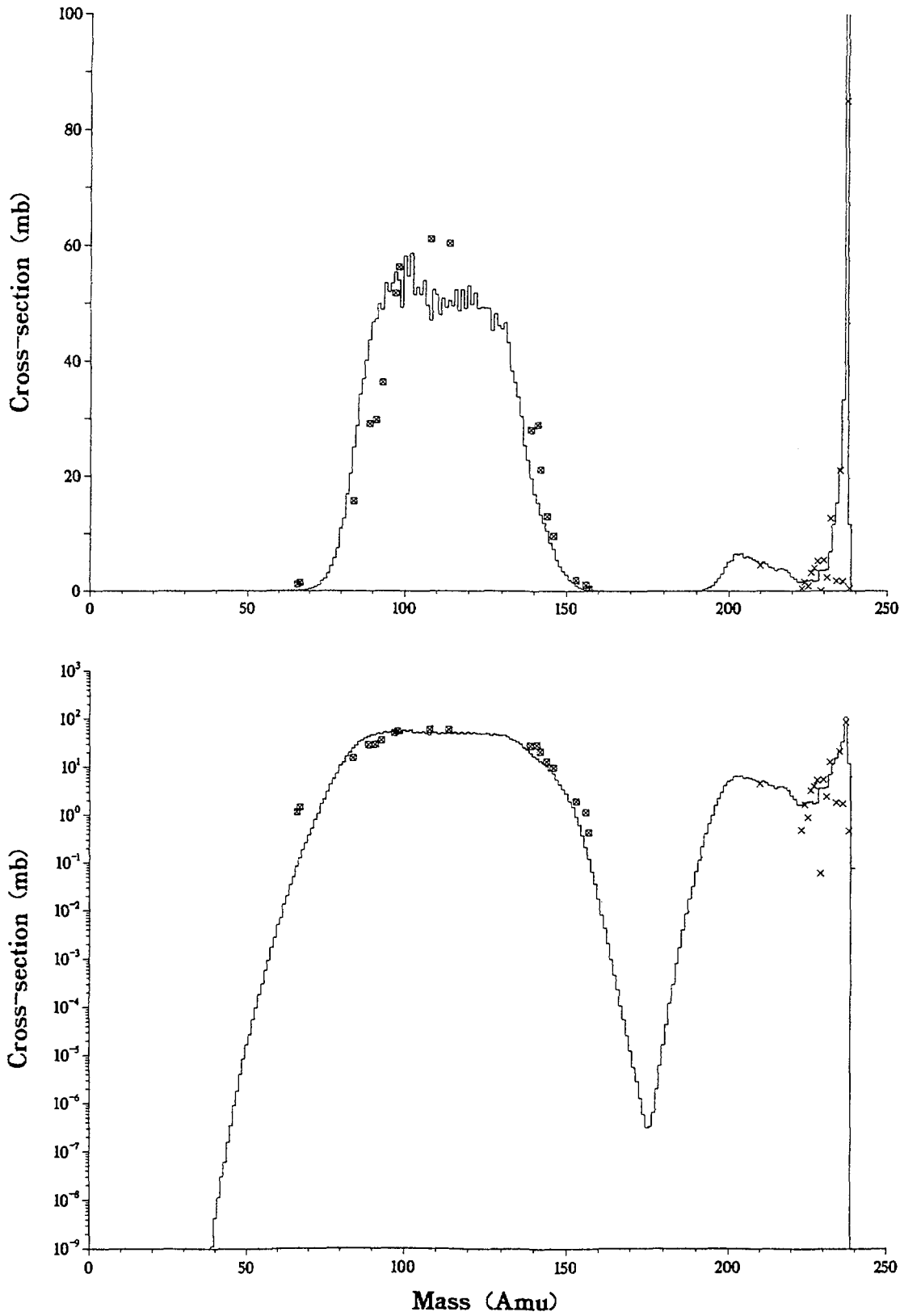


Figure 13: Calculated mass production cross-sections for 340 MeV proton interactions with ^{238}U . The experimental results for the fission masses are from Stevenson et al. [26] and for the spallation products from Lindner & Osborne [36].

Fission of ^{197}Au by 41.9 MeV Alphas

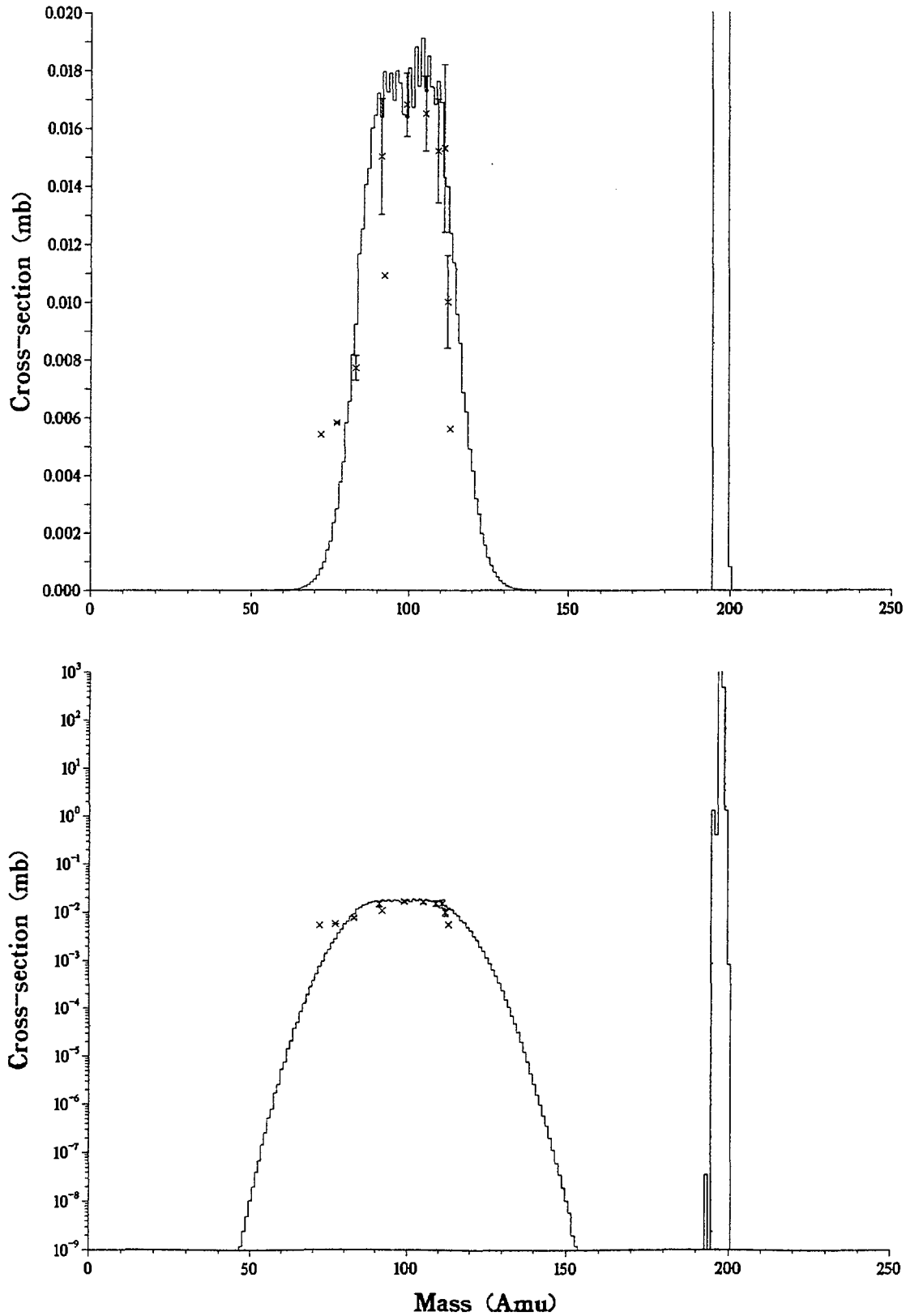


Figure 14: Calculated mass production cross-sections for 41.9 MeV α -particle bombardment of ^{197}Au . The experimental results (crosses) are from Neuzil & Fairhall [34].

Calculated and measured [36] production cross-sections (mb) for spallation products in 340 and 200 MeV proton interactions with ^{238}U .

340 MeV					
	Measurement	Calculation		Measurement	Calculation
^{238}Np	0.46 ± 0.05	4.8	^{236}Np	1.7 ± 0.1	2.8
$^{237}\text{U} + ^{237}\text{Pa}$	85	$73 + 33$	^{232}U	≤ 4	1.2
^{230}U	0.35 ± 0.12	0.12	^{229}U	0.06 ± 0.005	0.02
^{228}U	0.038 ± 0.002	0.0022	^{235}Pa	21 ± 2	7.1
^{232}Pa	8.7 ± 1	4.3	^{230}Pa	5.1 ± 0.5	1.6
^{228}Pa	1.7 ± 0.2	0.21	^{227}Pa	0.71 ± 0.06	0.074
^{234}Th	1.8 ± 0.7	0.85	^{231}Th	2.4 ± 0.1	1.0
^{228}Th	2.9 ± 0.9	1.5	^{227}Th	3.3 ± 0.4	1.4
^{226}Th	2.7 ± 0.2	1.5	^{228}Ac	0.62 ± 0.08	0.065
^{226}Ac	0.54 ± 0.09	0.37	^{225}Ac	0.62 ± 0.13	0.51
^{224}Ac	1.05 ± 0.05	0.85	^{228}Ra	0.043	0.016
^{225}Ra	0.26	0.041	^{224}Ra	0.58	0.12
^{223}Ra	0.48	0.26	^{210}At	1.2	2.1
^{210}Po	1.7	0.84	^{210}Bi	1.6	0.11
200 MeV					
	Measurement	Calculation		Measurement	Calculation
$^{237}\text{U} + ^{237}\text{Pa}$	67.5	$83 + 19$	^{230}U	0.41	0.17
^{229}U	0.1	0.023	^{228}U	0.03	0.0029
^{227}Pa	0.62	0.069	^{224}Ra	0.26	0.097
^{210}At	0.08	0.39	^{210}Po	0.17	0.21
^{210}Bi	1.1	0.02			

3.1 FUSSPOT

“Fission Under Spallation, Serber’s Physics On Top.”

This code handles the setting up for the de-excitation of the intermediate nuclei in medium energy nucleon interactions with heavy elements. The basic input is on a data file produced by MECC - the displacements in Z and N from the parent nucleus and excitation energy for each real event and at the end, after an E-O-F marker, the Z and A of the parent used, the Monte-Carlo statistics and the transport cross-section radius. These results (appropriately translated) are fed into EVAPF. The values are extended to the natural isotopic abundance using data tabulated in the data file STABLES.ASC and $A^{1/3}$ scaling of the nuclear radius. It is possible to use the MECC data set for a different element (if it is physically reasonable, eg Pb to Bi is acceptable but Pb to C is probably not a good idea).

One (optional) data record may be supplied:

ZT, AT, CXTOT, CXMIN, E_CALC nofpp auto

ZT: The charge to be used for the target nucleus

AT: The mass to be used for the target nucleus

CXTO: The total cross-section (mb) to be used OR if specified as a negative number this will be the radius (in fm) to be used to compute the transport cross-section.

CXMIN: Cross-sections below this value will be excluded from the output list.

E_CALC: The energy to be used in the output header (useful when building a data library of excitation functions!).

nofpp: If this keyword is specified (after any data), the processing for and of fission products will be bypassed - this can save huge amounts of computer time (several hours!).

auto: Supply this keyword if the job is to use the data at the back end of the MECC data set (e.g. use this keyword to setup a job to use the standard data when the “nofpp” is wanted).

The default in case no data is supplied (i.e. an End_of_file marker is the only input for FUSSPOT) is to use the information at the back of the MECC data set and to process the fission products as well.

3.2 PFMPH

This is a complimentary code to FUSSPOT, which makes evaporation/fission calculations on the basis of compound nucleus and the Optical-Model to compute the cross-section for the entrance channel.

The input data consist of one record (although several cases can be stacked one behind the other - if required)

Record 1: ZT, AT, IP, Elab, Emax, nofpp, spin, pem

ZT: The charge of the target nucleus.

AT: The mass of the target nucleus.

IP: The code for the incident particle - 1 neutron; 2 proton; 3 alpha; 4 deuteron

Elab: The laboratory kinetic energy (MeV) for the incident particle chosen.

E_{max}: Sets the upper limit (in MeV) for the excitation-energy grid for the calculation (As fission is exoergic, excitation energies for the scission fragments may exceed that of the scissioning nucleus).

nofpp. This keyword is supplied (after the numerical data) if the processing for fission products is to be skipped.

spin: If this keyword is supplied, angular momentum treated by the Lang prescription on an average basis will be included into the calculation.

pem: If this keyword is specified then a pre-equilibrium emission step using the hybrid model is inserted before the evaporation.

3.3 Notes on auxiliary routines

The entrance channel cross-section is calculated using the Optical-Model routines extracted from ALICE95 (OMINIT, OMCALC and TLJ). The OM calculation also returns the angular momentum distribution. If the 'spin' keyword is supplied, the excitation energy is reduced by the 'spin-energy' term on an average basis. The evaporation calculation does not take angular momentum change into account.

The hybrid pre-equilibrium emission model routine also comes from ALICE95 (HYBRID). For the specified target nucleus, incident particle and energy combination, it returns the excitation spectra for pre-equilibrium emission of 1xN, 1xP, 2xN, 2xP, 1xPN. The interface to the EVAPF package is carried out in subroutine HYBSET. This routine initializes the input values for HYBRID (HYBRID works in R*8, so part of this is simply type conversion) and then uses EVAPF2 calls to load the intermediate nuclei: Deduces the remaining compound nucleus entrance cross-section and the various excitation states for the (up to 6) 'PEM' nuclei.

A service routine (SETQCX) is used for some side-calculations; given the Z and A of the target nucleus and the incident particles code (IP), it calculates Q-values, etc. for the reaction, Z and A for the compound nucleus and makes the initialization call to OMINIT.

3.4 The EVAPF package

The evaporation/fission calculation is made with the EVAPF package of routines: Calls to EVFINI to set up the basic data, EVAPF1 to set up the specific calculation, EVAPF2 to load the various start nuclei and (finally) EVAPF to make the calculation. PUTOUT and GETP allow the retrieval of the residual nuclei.

The package is currently split into the following routines and entry points [EP]:

EVAPF1, [EP] EVAPF2, [EP] EVAP, EVAPFI, [EP] EVAPFP, [EP] EVFINI, PUT, [EP] PUTT, [EP] PUTF, [EP] PUTFP, [EP] PUTOUT, [EP] GETP, [EP] CLEARP, CLUSTR, EVAPF4, EVAPF6, EVAPF7, GPROB, BINDEN, ISORT, SORT.

These will be taken in a computationally logical order.

3.4.1 EVFINI

This is an ENTRY point of EVAPFI and makes the basic initializations of the nuclide mass data (MASS83F.DAT), the Cameron data (CAM.DAT) and actinide fission data (EVAPFD.DAT). Default values for some adjustable parameters are set.

MASS83F.DAT

Contains ASCII records with Z, A and the binding energy in MeV. The binding energies come from the 1983 mass evaluation together with extrapolated values (see Part II) so that the region +/- 15 masses about the estimated most stable for the isotope is covered.

CAM.DAT

An ASCII version of the Cameron data for shell and pairing energies versus Z and N as extracted from the old HETC data file.

EVAPFD.DAT

Contains fission data for the element region with Z from 88 to 100. An ASCII file with entries for 31 'A' values of the 13 elements, containing IZ & IA of the nucleus, the effective mean fission barrier (MeV), the effective neutron binding (MeV), the half separation between the two barriers (Note: These together with the mean barrier are consistent with a semi-classical solution of the two humped barrier - in particular, cases where a single barrier is more appropriate to the measured data are treated by moving one barrier sufficiently far away that its influence is negligible) and the ratio of the curvature energies of the two barriers.

3.4.2 EVAPF1

This subroutine is called with arguments specifying the highest Z, N and the minimum & maximum excitation energies to be used in the calculation. EVAPF1 initializes the energy bin structure and the various pointers for storage/manipulation of the nuclei. The routine can treat intermediate state nuclei spanning 32 units of charge (Z) and 40 in neutron number (N). This is sufficient for cases considered to date (the evaporation chain is continued outside these limits by EVAPF4 when necessary).

3.4.3 EVAPF2

EVAPF2 is called successively to load the required single nuclear states into the calculational arrays. Checks are made that the state actually fits in (a warning message is issued if it does not). The main calculational storage consists of 2 arrays with dimension 401 x 42 x 34, giving space for 401 excitation energy bins, 40 successive N-values and 32 Z-values. One array holds the statistical weights and the other the mean excitation energy.

The first energy bins can be wide - 3 or 4 MeV - as nuclei here cannot evaporate (by definition or coding) and is also the holding position for the end products of the calculation. The skin of the body of the box in the Z-direction for N= 41 & 42 and in the N-direction for Z= 33 & 34 are for passing the calculation on to EVAPF4 for completion.

Tallies of the nucleons and energy entering the calculation are kept so that conservation rules may be applied as a check. By setting a flag, each intermediate nuclear state can be made to undergo ONE evaporation cycle without any competition from fission if required.

3.4.4 EVAPF

EVAPF controls the actual evaporation calculation. It works down systematically from the highest Z, N and excitation energy, till all the nuclei are chased either to the [Z,N] periphery (and the calculation passed to EVAPF4 for completion) or the E* periphery (in which case all is complete!). The working arrays are systematically overwritten, as the calculation proceeds, with the data for the fissioning nuclei for passing to EVAPF7.

The run through the Zs, N's, E* for the parent, the 7 outcome probabilities and their spectra takes place in a set of nested loops. Calls to EVAPFI initialize the evaporation code for a particular [Z-N] state and EVAPFP then calculates the emission probabilities and particle spectra for the ejected

clusters and fission. Track is kept of gross energy changes and numbers of nucleons ejected (particle emission spectra, binding energy interchange, nucleon loss, etc). Products are written to accumulator arrays (via calls to PUTT and PUTF as appropriate)

In case of high excitation energies, the evaporation calculation is completed by EVAPF4. Before this, EVAPF7 is called to extract the fission products and after, EVAPF6 is called to de-excite the fission products. Optionally, the routine gives a full evaporation output at the end with particle and energy balance tables and the product formation probabilities.

Because of space problems, the main calculational storage has to be used several times. This involves some gymnastics with the arrays and carrying out the whole evaporation/fission/fission-product process in a specific order (controlled from EVAPF):-

- Before calling EVAPF7 (to produce the fission products), the Z/N peripheries are written to a temporary data set (for reading later in EVAPF4).
- EVAPF7 is called. It extracts the parameters for the *fissioning* nuclei from the main calculational arrays and writes them to a temporary data set, before using the same space as a buffer for the fission products.

EVAPF7 writes the fission products to a temporary data set for reading and processing by EVAPF6.

- EVAPF4 is called next and completes the evaporation calculation using two 4-deep lines (in the Z and N directions) and a 'corner' (which, again, overlay the main calculational arrays).
- EVAPF6 is called to process any fission products.

3.4.5 PUT & Co.

PUT, with three of its entry points (PUTT, PUTF and PUTFP) assemble product nuclei into a four-column stack. PUT is used for intermediate state nuclei with insufficient energy to evaporate anything, PUTT is for end states reached during the de-excitation, PUTF is for the fissioning nuclei and PUTFP for the fission products. Each call can extend the stack for all four types. The PUTF stack is used also for the treatment of the fission products (filled by EVAPFP and processed by EVAPF7) and PUTFP only used by EVAPF6.

PUTOUT lists all the products sorted into descending order by charge then mass and also gives a total production cross-section for each nuclide. GETP allows retrieval of the cross-section for a specific channel and CLEARP clears everything before the start of a new case.

3.4.6 EVAPF4

EVAPF4 makes the stage II de-excitation by working along two fronts and a corner. The new working arrays overlay those used by EVAPF. The re-arrangement is made by writing/reading to a temporary data set.

The calculation is split between 3 arrays:-

PZ N-front: 2 deep in N and NZMAX wide in Z (increases by 2 each time starting from NZTOP)

PN Z-front: 2 deep in Z and NNMAX wide in Z (increases by 2 each time starting from NNTOP)

PC Corner: Nuclides with Z of NZMAX+1, NZMAX+2 and N NNMAX+1 and NNMAX+2. Products are added from and to PZ/PN as appropriate.

One cycle of the de-excitation calculation gives N and Z reductions of 0, 1 and 2. Each iteration consists of two cycles through all three arrays:-

1. Evaporate PZ twice - this increases its length by 2.
2. Evaporate PN twice - length increases by 2.
3. Add the a's from PZ into the e's of PC.
4. Add the c's from PN into the e's of PC.
5. Evaporate PC twice - this increases by 2 in both the Z and N directions.
6. Add the g's from PC into the b's of PZ.
7. Add the f's from PC into the d's of PN.
8. For both PZ and PN, transfer row 3 to 1 and row 4 to 2.
9. For PC, move the h's to the g's.

The manipulations are summarised in Figure 15.

The calculation is the same as for EVAPF (calls to EVAPFI and EVAPFP etc.) but the 'empty' middle bit has been eliminated albeit at the expense of some array gymnastics. In this way, the whole range of Z (100) and N (150) can be covered. It is assumed that 1) no production of intermediate nuclei occur in this region and 2) no fission will occur in this range.

3.4.7 EVAPF6

This routine handles the de-excitation of the fission products. As even the most simple system involves lots of intermediate state nuclei, an adaptation of the EVAPF4 code is used.

The fission products are assembled in a temporary data set by EVAPF7, which also gives information on the highest Z, N and E*. EVAPF6 makes a first pass through the FP data set, accepting into the front corner calculational array (nnmax = nzmax = 0 otherwise products will be missed) those that will fit, checking and directly stuffing any products with insufficient energy to make evaporations and writing the residue to another T.D.S. Energy, nucleon etc. statistics are collected as appropriate for checking the balances through the calculation.

At the end of each cycle through the evaporation, the 'next' set of products that fit are added into the calculation (much simpler than the first pass as only reduced checking is required; this was all done on the first pass) and the residue sent to (another) T.D.S. (actually just two are used alternately).

The final residual nuclei are accumulated via PUTFP calls and particle emission statistics kept separately from those evaporated before fission. During the 1st pass through the T.D.S. the interchange statistics are accumulated and printed on the log file.

3.4.8 EVAPF7

EVAPF7 generates the scission products.

- 1) An algorithm to decide if scission is to be symmetric or asymmetric
- 2) Selects systematically the mass of the heavier product from distribution functions appropriate to the type of split. The cluster model distribution algorithm is in SUBROUTINE CLUSTR.
- 3) Selects the charge of the heavier product - Gaussian function of width 0.78 charge units about a mean selected on the basis of (roughly) equal displacement from stability for both products.
- 4) Calculates the probabilities for having excitation energy on the SAME energy grid as used in the initial evaporation phase on the basis of a Gaussian distribution of recoil kinetic energy.

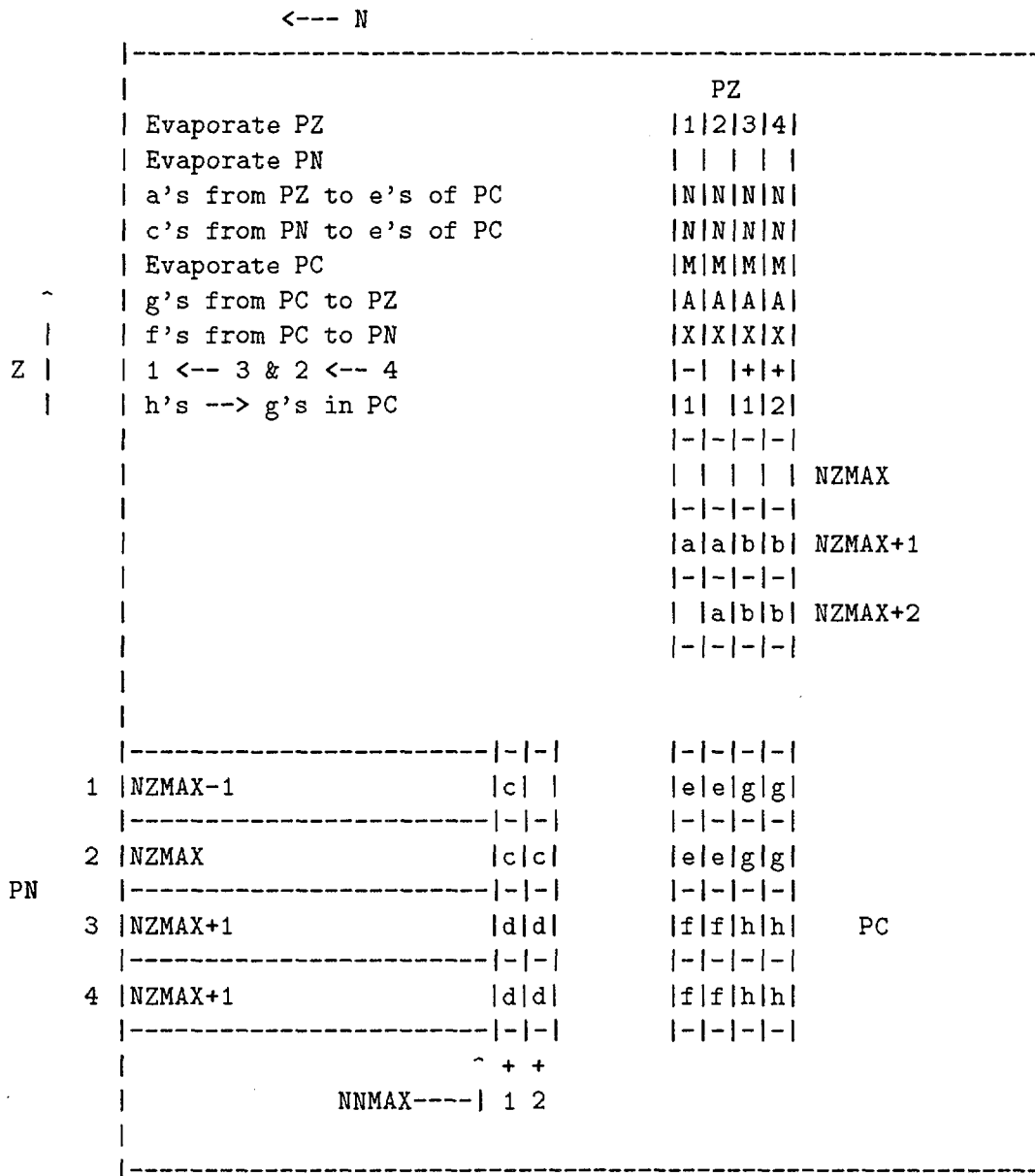


Figure 15: A summary of the data manipulations used to handle the evaporative de-excitation of the scission products.

- 5) Writes the scission products to an external data set.

The outermost loops are over the fissioning nuclei and their excitation - these are extracted from the CXP() accumulator array (filled by PUTF) and the P(, ,) and EMEAN(, ,) calculational arrays of EVAPFP and stored in a temporary data set. This is required as the scission products are assembled into a buffer that overwrites the P(, ,) and EMEAN(, ,) arrays.

The details of the parameters used for selecting the scission products may be seen in reference 13.

The gross interchange of binding energy, excitation energy and fragment recoil energy are accumulated. The maximum excitation energy, Z and N values are computed and returned to EVAPF6 in the argument list, to allow the initializations for the working arrays to be made.

3.4.9 Service routines

BINDEN: Function called by EVAPF7 with Z and A set to return the binding energy. Due to the complication of the logic of the routines, it was clearer to accept the overhead of the function call rather than in-line expansion as normally used.

GPROB: Function called by EVAPF7 to return the weight fraction of a Gaussian within given limits. The arguments are V1 & V2 the lower and upper limits of the integration (absolute values), VMEAN the mean value of the Gaussian and RSIGMA the reciprocal of root-2 times the standard deviation of the distribution. The routine uses a polynomial expansion for the complimentary error function.

ISORT: An indexed sorting algorithm for integers used by PUTOUT and EVAPF7.

SORT: A version of ISORT for floating point numbers.

Acknowledgment

I would like to thank R. Chawla and H.-U. Wenger for their helpful comments during the production of this report.

4 References

- 1 F. Atchison, "The PSIMECX medium-energy neutron activation cross-section library Part I: Description and usage procedures," Paul Scherrer Institut report No. 98-09 (1998)
- 2 F. Atchison, "The PSIMECX activation cross-section library Part-II: Computational methods for light to medium mass nuclei." Paul Scherrer Institut report No. 98-10 (1998)
- 3 F.D. Bechetti et al. Phys. Rev. 28C, 276 (1983)
- 4 V.P. Shamov, Paper P/2222, Proc. 2nd Geneva Conf. Peaceful use of Atomic Energy, Geneva 1958, Vol15, page 171
- 5 I Dostrovsky et al. Paper P/1615, Proc. 2nd Geneva conf. on the peaceful use of atomic energy, Vol 15, 301 (1958)
- 6 G. Rudstam and A.C. Pappas, Nucl. Phys. 22, 468 (1961)
- 7 V.S. Baraschikov et al., Dubna report, JINR P-1970 (1965)
- 8 F. Atchison, KfA Jülich meeting proceedings, Jül-Conf-34, 17 (1980)
- 9 F. Atchison, Proc. of specialists' meeting on intermediate energy nuclear data, OECD Issy-les-Moulineaux, France, May/June 1994, page 199
- 10 F.S. Alsmiller et al, Oak Ridge Nat. Lab. report, ORNL-TM-758 (1981)
- 11 H. Takahashi, Proc. Symp on neutron cross-sections from 10 to 50 MeV, Brookhaven Nat. Lab (1980)

- 12 Y. Nakahara Proc. 4th ICANS meeting, KEK Nat. Lab, Tsukuba, Japan, Oct 1980
- 13 F. Atchison, Paul Scherrer Institut report No. 98-12 (1998)
- 14 I. Dostrovsky, Z. Fraenkel, G. Friedlander, Phys. Rev. 116, 683 (1959)
- 15 I. Dostrovsky, Z. Fraenkel, L. Winsberg, Phys. Rev. 118, 781 (1960)
- 16 I. Dostrovsky, Z. Fraenkel, P. Rabinowitz, Phys. Rev. 118, 791 (1960)
- 17 R. Vandenbosch, J.R. Huizenga, Paper P688, Proc. 2nd UN Conf. on the peaceful uses of atomic energy, Geneva 1958, Vol 15
- 18 K. Wildermuth, Th. Kanellopelous, Nucl. Phys. 7, 150 (1958)
- 19 H. Faissner, K. Wildermuth, Nucl. Phys. 58, 177 (1964)
- 20 D.I. Garber et al. BNL-NCS-50496 (1975)
- 21 S.F. Mughabghab, D.I. Garber Brookhaven Nat. Lab report BNL-325 (1973)
- 22 R.W Lamphere, Nucl. Phys. 38, 561 (1962)
- 23 M.S. Moore, G.A. Keyworth Phys. Rev. C3, 1656 (1971)
- 24 H. Baba, S. Baba Nucl. Phys. A175, 199 (1971)
- 25 H.M. Steiner, J.A. Jungerman Phys. Rev. 101 807 (1956)
- 26 P.C. Stevenson, H.G. Hicks, W.E. Nervik, D.R. Nethaway Phys. Rev. 111, 886 (1958)
- 27 G.L. Bate, J.R. Huizenga Phys. Rev 133, 1471 (1964)
- 28 V.A. Kon'shin, E.S. Matusevitch, V.I. Regushevskii, Sov J. Nucl. Phys. 2, 489 (1966)
- 29 A.C. Pappas Z. Naturforschg. 21a, 995 (1966)
- 30 H.U. Wenger Private communication (1997)
- 31 L.G. Jodra, N. Sugarman, Phys. Rev. 99, 1470 (1955)
- 32 J.R. Boyce, T.D. Hayward, R. Bass, H.W. Newson, E.G. Bilpuch, F.O. Purser, H.W. Schmitt Phys. Rev. C10, 231 (1974)
- 33 E. Konecny, H.W. Schmitt Phys. Rev. 172, 1226 (1968)
- 34 E.F. Neuzil, A.W. Fairhall, Phys. Rev. 129, 2705 (1963)
- 35 S. Baba, H Umezawa, H. Baba Nucl. Phys. A175, 177 (1971)
- 36 M. Lindner, R.N. Osborne Phys. Rev. 103, 378 (1956)